

# Adiabatic CDM Models and the Competition

Lloyd Knox

*Department of Astronomy and Astrophysics, The University of Chicago  
5640 So. Ellis Avenue, Chicago, IL 60637-1433, USA*

*E-mail: [knox@flight.uchicago.edu](mailto:knox@flight.uchicago.edu)*

The inflation-inspired flat, cold dark matter-dominated models of structure formation with adiabatic, nearly scale-invariant initial conditions agree very well with current CMB anisotropy data. The success of these models is highlighted by the failure of alternatives; we argue that there are no longer any viable competitors (with the exception of models with more complicated matter content which are still flat and which still require inflation). CMB data will soon be of sufficient quality that, if one *assumes* inflation, one can detect a non-zero cosmological constant by combining a determination of the peak location with Hubble constant measurements.

## 1 Introduction

The aim of this paper is to demonstrate the success of inflation-inspired models of structure formation. The CMB data are pointing us towards models in which the mean spatial curvature is zero, and in which the “initial” perturbations were adiabatic and nearly scale-invariant. These three properties are all predictions of the simplest models of inflation. We will discuss them below and how they influence the properties of the CMB. Since we are never able to prove a model to be true, just that it is more probable than other models, much of the demonstration of the success of inflation-inspired models is a discussion of what goes wrong with other ones.

We begin with a very quick review<sup>1</sup> of the basics and then move on to a brief description of current data. The subsequent discussion of adiabatic models explains what adiabatic, flat and nearly scale-invariant mean and how these properties influence the CMB power spectrum. With this discussion complete we are then ready to see how isocurvature and defect models differ, and that they do so in ways that conflict with the data. Finally, the strong constraint on the peak location given all data, prompts a discussion about what we can learn from the peak location besides the geometry.

## 2 Preliminaries

At sufficiently early times, a thermal distribution of photons kept all the atoms in the Universe ionized. Because of the strength of the Thomson cross section

and the large number density of electrons, the photons were tightly coupled to the electrons (and through them to the nuclei) and therefore these components could be treated as a single fluid called the photon-baryon fluid. As the photon temperature cooled (due to the expansion of the Universe) below one Rydberg (actually well below one Rydberg due to the enormous photon-to-baryon ratio), the electrons combined with the nuclei thereby decoupling the photons from the baryons. The Universe became transparent to the photons that are now the CMB. Thus when we look at the CMB, we are seeing the Universe as it was at the time of decoupling—also referred to as “last-scattering”.

The temperature of the CMB is the same in all directions, to 1 part in 100,000. The most interesting statistical property of these tiny fluctuations is the angular power spectrum,  $C_l$ , which tells us how much fluctuation power there is at different angular scales, or multipole moments  $l$  (where  $l \sim \pi/\theta$ ). Because the departures from isotropy are so small, linear perturbation theory is an excellent approximation and the angular power spectrum can be calculated for a given model with very high precision. Thus the CMB offers a very clean probe of cosmology—one where the basic physics is much better understood than is the case for galaxies or even clusters of galaxies.

Throughout,  $\Omega_i$  is the mean density of component  $i$ ,  $\bar{\rho}_i$ , in units of the critical density which divides negatively and positively curved models. Note that  $\Omega \equiv \sum_i \Omega_i = 1$  corresponds to the case of zero mean spatial curvature.

### 3 The Data

The last year of the 1000’s was a very exciting one for those interested in measurements of the angular power spectrum. New results came from MSAM<sup>2</sup>, Python<sup>3,4</sup>, CAT<sup>5</sup>, MAT<sup>6,7,8</sup>, IAC<sup>9</sup>, Viper<sup>10</sup>, and BOOM/NA<sup>11</sup>, all of which have bearing on the properties of the peak. These data make a convincing case that we have indeed observed a peak—which not only rises towards  $l = 200$  (as we have known for several years<sup>12</sup>) but also falls dramatically towards  $l = 400$ . Figure 1 shows the results from 1999 plus, in background shading, a fit<sup>13</sup> of the power in 14 bands of  $l$  to all the data. Many of the bands are at low enough  $l$  that they cannot be discerned on a linear x-axis plot. The  $\Omega = 1$  model in the figure has a mean density of non-relativistic matter,  $\Omega_m = 0.31$ , a cosmological constant density of  $\Omega_\Lambda = 0.69$ , a baryon density of  $\Omega_b = 0.019h^{-2}$ <sup>29</sup>, a Hubble constant of  $H_0 = 100h$  km/sec/Mpc with  $h = 0.65$ , an optical depth to reionization of  $\tau = 0.17$  and a power spectrum power-law index of  $n = 1.12$ , where  $n = 1$  is scale invariant.

Knox and Page<sup>14</sup> have recently characterized the peak with fits of phenomenological models to the data. They find the peak to be localized by

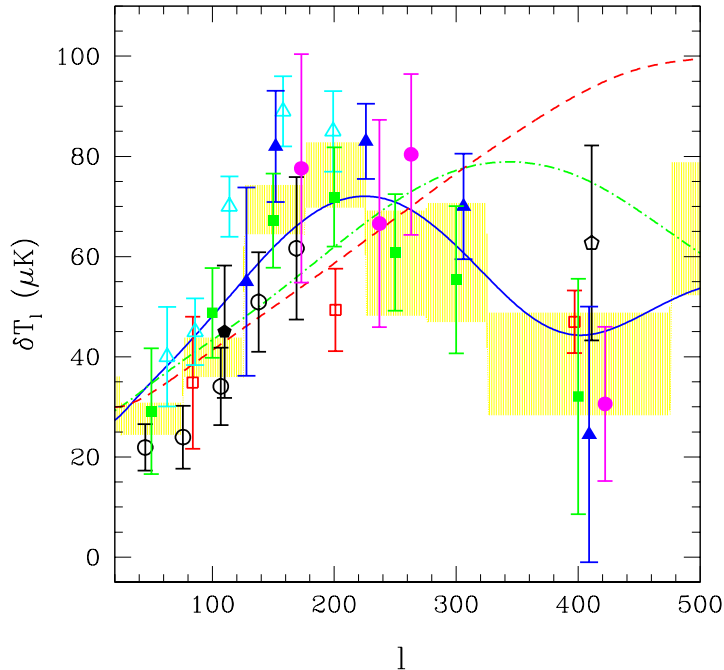


Figure 1: Bandpowers from TOCO97 (cyan open triangles), TOCO98 (blue filled triangles), BOOM/NA (green filled squares), MSAM (red open squares), CAT (black open pentagon), IAC (black filled pentagon), PyV (black open circles) and Viper (green filled circles). The y-axis is  $\delta T_l \equiv \sqrt{l(l+1)C_l}/(2\pi)$  where  $C_l$  is the angular power spectrum. The models are (from peaking at left to peaking at right) the best fit models of<sup>17</sup> for  $\Omega = 1$ ,  $\Omega = 0.4$  and  $\Omega = 0.2$ . Calibration errors are not shown.

TOCO and BOOM/NA at  $175 < l_{\text{peak}} < 243$  and  $151 < l_{\text{peak}} < 259$  respectively (both ranges 95% confidence). This location is also indicated by combining the PythonV and Viper data, as can be seen in Fig. 1 and a significant bound can also be derived by combining all other data, prior to these four data sets. In sum, a peak near  $l \sim 200$ , is robustly detected. Combining all the data, we can also constraint its full-width at half-maximum to be between 180 and 250 at 95% confidence.

## 4 Physical Models

In this section we describe three classes of physical models (adiabatic CDM, topological defects and isocurvature dark matter) and their predictions for the angular power spectrum<sup>15</sup>.

### 4.1 Adiabatic CDM

The simplest models of inflation lead to a post-reheat Universe with critical density (to exponential precision) and adiabatic, nearly scale-invariant fluctuations<sup>16</sup>. Although inflation does not require cold dark matter, the prediction of critical density, combined with upper limits on the mean baryonic density, push one in that direction. Within the last few years, the observations have developed to strongly prefer the gap between  $\Omega_b$  ( $b \equiv$  baryons) and

unity to be filled with not just cold dark matter, but a sizeable helping of dark energy too, e.g.,<sup>17,18,19,28</sup>. Let's examine more precisely each of these three predictions.

### Adiabatic

Adiabatic (or, equivalently, isentropic) means that there are no spatial fluctuations in the total entropy *per particle of each type*. That is,  $\delta(s/n_i) = 0$  for all species  $i$ . From this, we see that  $\delta n_i/n_i = \delta s/s$  and therefore all species have the same fractional fluctuation in their number densities. For example, where there are more dark matter particles there are more photons, etc. A general perturbation<sup>20</sup> is a linear combination of isocurvature and adiabatic modes. Isocurvature perturbations are arranged so that  $\delta\rho = \sum_i \delta\rho_i = 0$ .

The evolution of a single Fourier mode is initially a competition between the pressure of the baryon-photon fluid trying to decrease density contrasts, and gravity trying to enhance them. For adiabatic modes the gravitational term is initially dominant, increasing the amplitude of the mode, until the restorative force of the pressure gradients pushes it back. Despite the initial growth in the density contrast, the potential decays. This is because the photon pressure prevents the growth from happening quickly enough to counteract the effects of the expansion. It is this decay of the potential that leads to excitation of a cosine mode (after the initial transient) for the acoustic oscillation. For isocurvature modes, the potential is initially zero, until there is sufficient time for pressure gradients to evolve into density gradients. The initially growing potential excites a sine mode<sup>21,22</sup>.

All adiabatic modes of given wavenumber,  $k = \sqrt{k_x^2 + k_y^2 + k_z^2}$ , although they have different *spatial* phases, will all have the same *temporal* phase, because they all start off with the same relationship between the dark matter and photons. In other words, although spatially incoherent, they are temporally coherent. This coherence is essential to the familiar Doppler peak structure of the CMB power spectrum<sup>23</sup>. Figure 2 illustrates the point by showing the spatial dependence of three different modes with varying wave numbers at five different stages of their evolution.

### Flat

Inflation generically produces flat Universes—ones where the mean spatial curvature is exponentially close to zero (e.g.,  $e^{-100}$  is a particularly large residual curvature). The CMB is sensitive to curvature because the translation of a linear distance on the last-scattering surface to an angular extent on the sky

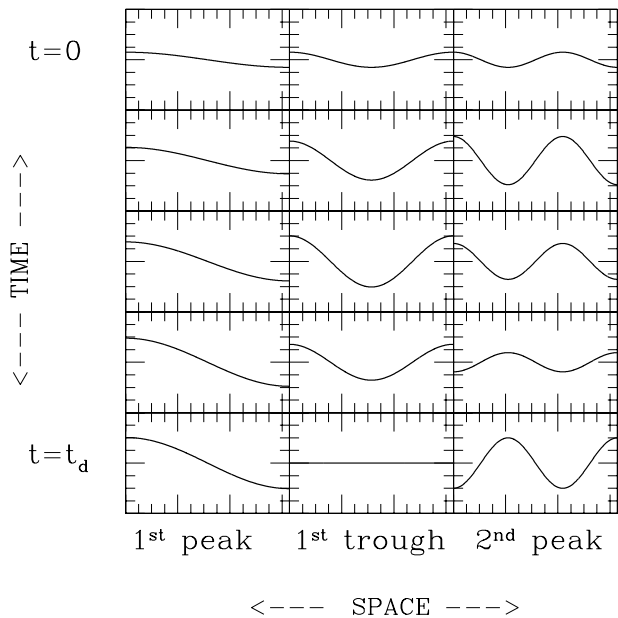


Figure 2: Spatial dependence of the photon-baryon fluid temperature for three different modes at five different times. Shown is the evolution from very early when the wavelengths are much larger than the Hubble radius and causal processes have not had time to change the “initial conditions” as left by inflation (top panels) to the time of decoupling between matter and radiation (bottom panels). The longest wavelength mode is shown on the left. It reaches its first maximum just at the time of decoupling. The peak-to-trough distance, as seen by us today, subtends about a degree on the last-scattering surface. The fact that this mode (and all modes with the same wavelength) reach an extremum just at the time of decoupling is the reason for the first peak in the CMB power spectrum at  $l \sim 200$ . Contrast this behavior with that of a mode with half the wavelength (shown in the five middle panels) which therefore oscillates in time twice as fast and hits a null at the time of decoupling. Modes like this one have a peak-to-trough distance of about half a degree and are responsible for the first trough at  $l = 400$ . Finally, the right-most panels are for the even faster and shorter modes responsible for the second peak.

depends on it. One can see this by noting that in a negatively curved space the surface area of a sphere of radius  $r$  is larger than  $4\pi r^2$  and therefore objects at fixed coordinate distance of fixed size appear smaller than they would in the case of zero curvature (the larger-than- $4\pi r^2$  sphere must be squeezed into a local  $4\pi$  steradians). This geometrical effect shifts the CMB power spectrum peak locations by a factor of  $\Omega^{-1/2}$ . Other parameters also affect the peak locations by altering the coordinate distance to the last-scattering surface and the size of features there; these are subdominant effects which will be discussed later.

### Nearly Scale Invariant

The power spectrum of fluctuations produced by the simplest models of inflation is well-described by a power law,  $P(k) \propto k^n$ , with  $n$  near unity. The case  $n = 1$  is called scale-invariant because the dimensionless quantity  $k^3 P(k)$  is the same for all modes when the comparison is done at “horizon crossing” (when the mode wavelength becomes smaller than the Hubble radius)<sup>16</sup>.

## 4.2 Topological Defects

The usual scenario for topological defects is that a phase transition in an initially homogeneous Universe gives rise to a scalar field with a spatially-varying stress-energy tensor. In most such scenarios, the scalar field configuration evolves into a network of regions which are topologically incapable of relaxing to the true ground state. Causality implies that these models have isocurvature initial conditions.

In defect models, the temporal coherence is lost due to continual sourcing of new perturbations by the non-linearly evolving scalar field. This generically leads to one very broad peak with a maximum near  $l = 400 - 500$ <sup>23</sup>. Thus the drop in power from  $l = 200$  to  $l = 400$  is a very challenging feature of the data. One can get lower power at  $l = 400$  than at  $l = 200$  with modifications to the ionization history<sup>24</sup>, but even for these models the drop probably is not fast enough. See A. Albrecht's contribution to these proceedings.

## 4.3 Isocurvature Dark Matter Models

Note that isocurvature is more general than adiabatic. Given numerous components, there are a number of different ways of maintaining the isocurvature condition,  $\sum_i \delta\rho_i = 0$ . In what follows we will assume that the isocurvature condition is maintained by the dark matter compensating everything else.

Isocurvature models have at least two strikes against them. First, scale-invariant models produce far too much fluctuation power on large angular scales, when normalized to galaxy fluctuations at smaller scales as has been known for over a decade<sup>25</sup>. One might hope to save isocurvature models by tilting them far from scale invariant, but this fix cannot simultaneously get galaxy scales, COBE-scales and Doppler peak scales right.

The second strike has to do with the location of the acoustic peaks. As mentioned above, the isocurvature oscillations are 90 degrees out of phase with the adiabatic ones. The peaks get shifted to *higher*  $l$  ( $l = 350$  to  $400$  for the first peak)<sup>22</sup>. Geometrical effects could shift it back, to make it agree with the data, but this would require  $\Omega > 2$  which is inconsistent with a number of observations<sup>15</sup>.

There are scenarios with initially isocurvature conditions that can produce CMB power spectra that look much like those in the adiabatic case. This can be done by adding to adiabatic fluctuations, another component which maintains the isocurvature condition and then by giving this extra component a non-trivial stress history<sup>30</sup>. These alternatives will be interesting to pursue further if improvements to the data cause troubles for the currently successful adiabatic models. Even these alternatives are flat models that require some

mechanism, such as inflation, for creating the super-horizon correlations in their initial conditions.

Turok has shown that even super-horizon correlations are not a necessary condition for CMB power spectra that mimic those of inflation<sup>31</sup>. Although no specific model is constructed, this work demonstrates that causality alone does not preclude one from getting inflation-like power spectra without inflation. For a discussion of the physical plausibility of models that could do this, see <sup>32</sup>.

## 5 Peak Location and $\Omega_\Lambda$

If we *assume* flatness, adiabaticity and near scale-invariance we can then determine  $\Omega_\Lambda$  from the location of the first peak<sup>33</sup>. With these assumptions, the peak position just depends on the coordinate distance to the last-scattering surface divided by the sound horizon at last-scattering. How this ratio depends on  $\Omega_\Lambda$  depends on what else we hold fixed. If we have high-precision CMB data over several peaks then  $w_b \equiv \Omega_b h^2$  and  $w_c \equiv \Omega_c h^2$  would be good things to keep fixed, since those are what affect the acoustic peak morphology<sup>26</sup>. However, without such high precision data,  $w_b$  and  $H_0$  are good things to fix because we know these fairly well from other measurements. With  $w_b$  and  $H_0$  fixed, increasing  $\Omega_\Lambda$  increases the sound horizon (because  $w_c$  must decrease) but increases the coordinate distance to the last-scattering surface by more and the peak moves out to higher  $l$ . With  $w_b$  and  $w_c$  fixed, the sound-horizon stays the same but  $H_0$  increases and the coordinate distance to the last-scattering surface drops: the peak shifts to lower  $l$ .

If we take all the data, the peak location is  $l_{\text{peak}} = 229 \pm 9^4$ . Thus, if we assume  $h = 0.65$  then this is evidence for a positive cosmological constant. It is weak evidence because inclusion of possible systematic errors would probably widen the peak bound significantly. However, for a sample-variance dominated measurement of the first peak (specifically,  $C_l$  from  $l = 100$  to  $l = 300$ ) derived from observations of 1000 square degrees of sky (comparable to the Antarctic Boomerang coverage) one can determine the peak to be at, e.g.,  $l_c = 220 \pm 5$ . One can see from Fig. 5 that we may soon have a strong determination of non-zero  $\Omega_\Lambda$  based solely on Hubble constant and CMB measurements. Note that this determination will not suffer from calibration uncertainty.

## 6 Conclusion

The peak has been observed by two different instruments, and can be inferred from an independent compilation of other data sets. The properties of this

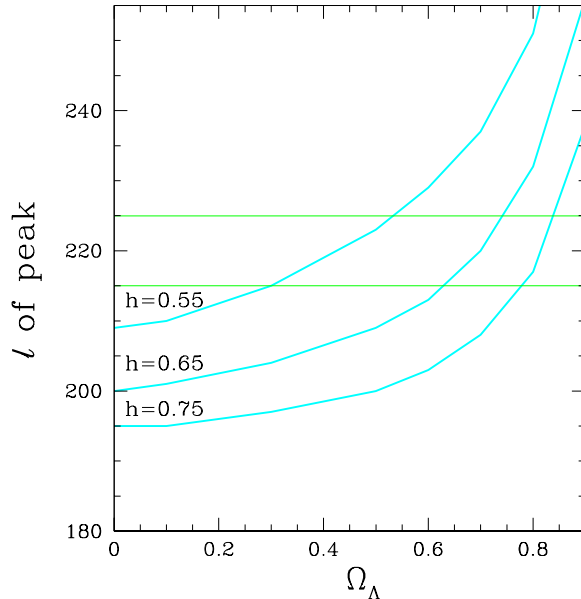


Figure 3: We find  $l_{\text{peak}}$  as we vary  $\Omega_\Lambda$  for three values of the Hubble constant. We always fix  $\Omega_b h^2 = 0.019$ , no reionization, no gravity waves, no tilt. The horizontal lines show  $1\sigma$  constraint on  $l_{\text{peak}}$  of  $220 \pm 5$  that should be possible from Boom98 data, just using  $100 < l < 300$ . The corresponding bound for MAP will be about  $\pm 1$ .

peak are consistent with those of the first peak in the inflation-inspired adiabatic CDM models, and inconsistent with competing models, with the possible exception of the more complicated isocurvature models mentioned above. It is perhaps instructive that where the confrontation between theory and observation can be done with a minimum of theoretical uncertainty, the adiabatic CDM models have been highly successful.

### Acknowledgments

I thank A. Albrecht, L. Page and J. Ruhl for useful conversations and D. Eisenstein for comments on the manuscript. I used CMBAST<sup>34</sup> and am supported by the DoE, NASA grant NAG5-7986, and NSF grant OPP-8920223.

### References

1. For a longer review, see M. White, D. Scott and J. Silk, Annual Review of Astronomy and Astrophysics, **32**, 315 (1994). For a textbook treatment see, e.g., P.J.E. Peebles, “Principles of Physical Cosmology”, Princeton University Press, Princeton, NJ (1993).
2. G. Wilson, *et. al.* 1999, astro-ph/9902047.
3. K. Coble et al., Astrophys. J. **519**, L5 (1999) (astro-ph/9902195)
4. K. Coble, Ph.D. Thesis, astro-ph/9911419.
5. J. C. Baker et al., Submitted to MNRAS, astro-ph/9904415.



6. E. Torbet *et al.* *Astrophys. J.* **521** L79 (1999)(astro-ph/9905100)
7. A. Miller *et al.*, *Astrophys. J.* **524** L1 astro-ph/9906421.
8. The Mobile Anisotropy Telescope (MAT) has produced two data sets referred to as TOCO97 & TOCO98, or TOCO collectively.
9. Dicker *et al.* Submitted to MNRAS 1999. (astro-ph/9907118)
10. J. B. Peterson *et al.*, astro-ph/9910503.
11. P. D. Mauskopf *et al.*, astro-ph/9911444.
12. D. Scott and M. White, astro-ph/9407073, Proceedings of the CWRU CMB Workshop ‘2 years after COBE’ eds. L. Krauss & P. Kernan (1994).
13. J.R. Bond, A.H. Jaffe and L. Knox, *Astrophys. J.* in press, astro-ph/9808204 (1998).
14. L. Knox and L. Page, astro-ph/0002162.
15. For further discussion of the implications of CMB data, see D. Scott and M. White, *Publ.Astron.Soc.Pac.* **111**, 525 (1999), astro-ph/9810446 and references therein..
16. For a textbook treatment of inflation, see, e.g., E.W. Kolb and M.S. Turner, “The Early Universe”, Addison-Wesley, New York, NY (1990).
17. Dodelson, S. & Knox, L., 1999, astro-ph/9909454.
18. Bahcall, N., Ostriker, J. P., Perlmutter, S., and Steinhardt, P. J., 1999, *Science*, 284, 1481-1488 (astro-ph/9906463);
19. M.S. Turner, “The Third Stromlo Symposium: The Galactic Halo”, eds. B.K. Gibson, T.S. Axelrod and M.E. Putman, ASP Conference Series **165**, 431 (1999); astro-ph/9811454.
20. We are here restricting ourselves to a two-component description (dark matter and baryon-photon fluid). With more components, there may be more modes. See M. Bucher, K. Moodley and N. Turok, astro-ph/9904231.
21. W. Hu and N. Sugiyama, *Phys. Rev. D* **51**, 2599 (1995).
22. W. Hu and M. White, *Astrophys. J.* **471**, 30 (1996).
23. e.g., J. Magueijo, A. Albrecht, P. Ferreira and D. Coulson, *Phys. Rev. D* **54**, 3727 (1996).
24. J. Weller, R.A. Battye and A. Albrecht, *Phys.Rev. D* **60**, 103520 (1999).
25. G. Efstathiou and J. R. Bond, *MNRAS* **218**, 103 (1986).
26. G. Efstathiou and J. R. Bond, *MNRAS* **304**, 75 (1999).
27. See e.g., J.R. Mould *et al*, astro-ph/9909260.
28. A.G. Riess, *et al.*, *Astron. J.* **116**, 1009 (1998); S. Perlmutter *et al*, *Astrophys. J.* **517**, 565 (1999) (astro-ph/9812133).
29. S. Burles, K. N. Nollett, J. M. Truran, M. S. Turner, *Phys. Rev. Lett.* **82** 4176 (1999).
30. W. Hu, *Phys. Rev. D* **59**, 121301 (1999); W. Hu, P.J.E. Peebles, astro-

- ph/9910222.
31. N. Turok, Phys. Rev. Lett. **77**, 4138 (1996).
  32. W. Hu, D. Spergel and M. White, Phys. Rev. **D55**, 3288 (1997).
  33. Or, from the second peak: M. Kamionkowski and A. Buchalter, astro-ph/0001045
  34. U. Seljak & M. Zaldarriaga, Astrophys. J. **469**, 437 (1996).